Vertical structure of stratospheric water vapour trends derived from merged satellite data

M. I. Hegglin[1,*], **D. A. Plummer**[2], **T. G. Shepherd**[1], **J. F. Scinocca**[2], **J. Anderson**[3], **L. Froidevaux**[4], **B. Funke**[5], **D. Hurst**[6], **A. Rozanov**[7], **J. Urban**[8], **T. von Clarmann**[9], **K. A. Walker**[10], **H. J. Wang**[11], **S. Tegtmeier**[12], and **K. Weigel**[7]

[1]University of Reading, Department of Meteorology, Reading RG6 6BB, UK

[2]Canadian Centre for Climate Modelling and Analysis, Victoria, British Columbia V8W 3V6, Canada

[3]Hampton University, Atmospheric and Planetary Science, Hampton, Virginia 23668, USA

[4]Jet Propulsion Laboratory, California Institute of Technology, Pasadena, California 91020, USA

[5]Instituto de Astrofisica de Andalucia, Granada 18008, Spain

[6]NOAA Earth System Research Laboratory, Global Monitoring Divison, Boulder, Colorado 80305, USA

[7]University of Bremen, Institute of Environmental Physics, Bremen 28334, Germany

[8]Chalmers University of Technology, Department of Earth and Space Sciences, Gothenburg, 412 96, Sweden

[9]Karlsruhe Institute of Technology, Karlsruhe 76021, Germany

[10]University of Toronto, Toronto M5S 1A7, Canada

[11]Georgia Institute of Technology, School of Earth and Atmospheric Sciences, Atlanta, Georgia 30332-0340, USA

[12]GEOMAR, Kiel 24105, Germany

Abstract

Stratospheric water vapour is a powerful greenhouse gas. The longest available record from balloon observations over Boulder, Colorado, USA shows increases in stratospheric water vapour concentrations that cannot be fully explained by observed changes in the main drivers, tropical tropopause temperatures and methane. Satellite observations could help resolve the issue, but

constructing a reliable long-term data record from individual short satellite records is challenging. Here we present an approach to merge satellite data sets with the help of a chemistry-climate model nudged to observed meteorology. We use the models' water vapour as a transfer function between data sets that overcomes issues arising from instrument drift and short overlap periods. In the lower stratosphere, our water vapour record extends back to 1988 and water vapour concentrations largely follow tropical tropopause temperatures. Lower and mid-stratospheric long-term trends are negative, and the trends from Boulder are shown not to be globally representative. In the upper stratosphere, our record extends back to 1986 and shows positive long-term trends. The altitudinal differences in the trends are explained by methane oxidation together with a strengthened lower-stratospheric and a weakened upper-stratospheric circulation inferred by this analysis. Our results call into question previous estimates of surface radiative forcing based on presumed global long-term increases in water vapour concentrations in the lower stratosphere.

Recent experiences with climate data records suggest that there is nothing like 'the ultimate climate data record' and that different approaches to data set construction are needed to estimate the uncertainty introduced by the construction process itself. For example, upper-tropospheric warming was underestimated by Microwave Sounding Unit Channel 2 temperature owing to the influence of a priori information and the coarse vertical resolution of the retrieval[1]. More recently, it has been argued[2] that the apparent hiatus in global-mean warming is an artefact of sampling biases in the global network of surface data used to estimate global mean temperature changes. Both examples illustrate the limitations of observational data sets with gaps filled by statistical relationships.

An important climate data record is stratospheric water vapour, which exerts a strong radiative forcing affecting temperatures both locally[3] and at Earth's surface[4,5]. Through thermal-wind balance, stratospheric temperature changes are believed to affect the stratospheric circulation and, through dynamical coupling, surface climate[6,7]. Long-term changes in extratropical lower-stratospheric water vapour derived from balloon measurements at Boulder (the longest available record[8]) from 1980 to 2010 show an average increase of 1.0 ± 0.2 ppmv in the 16–26 km altitude range[9,10]. About 25–30% of this increase has been attributed to methane oxidation[10,11]. The rest remains unexplained, as tropical tropopause temperatures (another key driver of long-term changes[12]) exhibit trends that are not significantly different from zero over this period[13,14]. Comparison of the Boulder record with HALOE satellite measurements, which exhibit an essentially zero long-term trend from 1992 to 2005, shows discrepancies in the early 1990s[15]. However, there is a possibility that the HALOE record suffers from aerosol contamination or long-term drifts[16].

The observed records of stratospheric water vapour thus present a conundrum. As a result, confidence in global long-term trends is low[17,18]. The difficulty in quantifying stratospheric water vapour trends arises from limitations of observational systems in the face of strong interannual and decadal variability[15,19,20]. There is general agreement that upper-tropospheric and lower-stratospheric humidity measurements from the global radiosonde network cannot be trusted[21]. Balloon-borne frostpoint hygrometers are characterized by high accuracy and precision[22], but their measurement records are temporally and spatially sparse. Satellite instruments offer global coverage but have finite lifetimes, so different data sets

need to be merged into long-term records, often without much overlap. Even with overlapping data sets, the merging may introduce temporal inhomogeneities because ageing instruments can show degradation in performance.

New approach to merge satellite data sets

We introduce a new approach to investigate long-term trends in stratospheric water vapour, using time series from a state-of-the-art chemistry–climate model nudged to observed meteorology (but not water vapour) from the ERA-Interim reanalysis over 1980–2010 (CMAM30) as a transfer function between satellite data sets. This approach exploits the extensive effort made in developing stable reanalysis products, with ERA-Interim now exhibiting a much better representation of the stratospheric circulation than earlier products[21]. The resulting CMAM30 stratospheric water vapour is expected to provide a reasonable long-term reference as it includes the main known transport, mixing, microphysical (dehydration at the tropical tropopause) and chemical processes (in particular methane oxidation) affecting its distribution and long-term changes. Although the model is not assumed to be correct in absolute terms, its use as a transfer function allows relative biases between satellite instruments to be determined using all available measurements, not just those restricted to overlap periods, thereby improving the characterization of inter-instrument biases and allowing the identification of potential instrumental drifts or sampling issues. Consistency between model and measurements suggests that the processes controlling stratospheric water vapour are sufficiently well understood to explain the long-term changes, and that CMAM30 can be trusted as a transfer function, whereas inconsistencies point out weaknesses either in the model or observations. The temporal homogeneity of the water vapour record can also be tested by examining the consistency of its long-term changes with those of other variables. Using this knowledge, the observational data sets can more confidently be used to create long-term data records.

As an application of the approach, we merge zonal monthly-mean water vapour time series from seven limb-viewing satellite instruments, compiled and quality assessed by the SPARC Data Initiative[23] into a long-term record. Figure 1a shows the individual satellite time series at 100 hPa for 20° S–20° N and the large discrepancies between them. Relative biases to CMAM30 are calculated for each instrument (Fig. 1b), avoiding periods where the instruments have known problems (Supplementary Methods). The post-2006 period is excluded from the relative-bias calculation because of a known inhomogeneity in ERA-Interim lower-stratospheric temperatures in late 2006 due to the introduction of GPS radio-occultation data[24] (Supplementary Methods and Supplementary Table 1). Overall, the relative biases are seen to be well defined (as shown in scatter plots in Supplementary Fig. 1), yielding confidence in the ability of CMAM30 to represent water vapour variability, and thus in its use as a transfer function between data sets. Using CMAM30 as a transfer function, each instrument record is then adjusted relative to Aura-MLS (Fig. 1d).

There is a potential pitfall in this approach in that long-term changes in the merged data set could be influenced by the long-term trend in the model. This possibility is assessed by examining whether there are apparent drifts in the model-measurement differences over time, or jumps between the older (SAGE II and HALOE) and newer instruments following

the bias correction (Fig. 1c). For the most part, the differences between these bias-corrected time series and CMAM30 are stable in time, suggesting that there is no artificial long-term trend introduced by this procedure. That the differences are stable over the SAGE II record furthermore indicates very good long-term stability of these observations, despite earlier concerns about a drift in the instrument's retrieval channel[25]. This suggests that SAGE II can be used to extend the satellite water vapour record back to the mid 1980s. Distinct low biases are found for HALOE during 1993–1995, which are probably due to aerosol interference in the retrieval after the Mt. Pinatubo eruption, and during 2003–2005, confirming previous comparisons[16,20]. Similarly, the last year of SAGE II data (2005) seems to exhibit a low bias. The earlier MIPAS data (2002–2004) indicate a slight low bias with respect to the later MIPAS data (2005–2010), as also found in ref. 23. The remaining fluctuations reveal mostly differences in how the instruments resolve the amplitude of the seasonal cycle, probably attributable to differing vertical resolutions of the observations[23]. The bias-corrected time series show a coherent evolution of tropical lower-stratospheric water vapour (Fig. 1d), with no evidence of a jump between the older and newer instruments —further evidence that the procedure has not introduced any artificial long-term trend. A merged satellite stratospheric water vapour record is finally produced by calculating the multi-instrument mean of all available bias-corrected data sets (however, excluding HALOE during 2003–2005 and SAGE II during 2005 owing to their identified low biases).

Consistency with tropical tropopause temperatures

In the lower stratosphere, water vapour is known to broadly follow variations in tropical tropopause temperatures[15–17,19,20,26–28]. The merged record is therefore compared to temperature fluctuations, using deseasonalized anomalies normalized by the standard deviation of the respective variable's interannual variability to make them comparable and check their consistency (Fig. 2a). We here use the CMAM30 100 hPa temperature averaged over 15° S–15° N, which has been shown to vary coherently with cold-point tropopause temperatures[19,28], and emphasize again that the variability and trends of the individual data sets are unaffected by the bias correction and thus not influenced by the model. The 80 hPa water vapour anomalies derived from the merged satellite record (at this level representative of purely stratospheric air) strongly follow the temperature fluctuations, with a correlation coefficient (R) (or variance explained) of 0.77 (59%) over the full time period, which increases to 0.89 (78%) when considering only 2001 onwards (probably explained by the better spatio-temporal coverage provided by the newer instruments, resulting in more representative zonal monthly means). The consistency between the temperature and water vapour data sets is further highlighted by plotting the normalized differences (or residuals) of their anomalies (Fig. 2b,c), for which the interannual variability is much reduced.

Consistency between the merged water vapour record and tropical tropopause temperatures is also found in the extratropical lower stratosphere at 100 hPa (with a lag of two months to account for transport timescales between the tropics and extratropics[28]; Fig. 2d,e), with a correlation coefficient (variance explained) of 0.66 (43%). The normalized differences between water vapour and temperature are somewhat stronger than in the tropics, owing to enhanced dynamical variability and its effect on tracer transport and mixing with older stratospheric air at these latitudes. Dehydration in the polar vortex may also contribute[29].

The good agreement between measurements and model (Fig. 2e) shows that these additional processes are adequately represented in the model. Nevertheless, the low-frequency variability of extratropical lower-stratospheric water vapour seems mainly to arise from the variability of tropical tropopause temperatures.

There are four time periods that show deviations from this strong correlation: 1992–1996 for the observations (but not for the model), which is presumed to be a result of Mt Pinatubo aerosol affecting the water vapour retrieval[16]; and 1999–2000, 2003 and 2008–2009. The causes of the latter are not known but because they occurred in both observations and model they are presumed to be real.

The new merged water vapour record seems to be an improvement over a previous merge of the HALOE and Aura-MLS data sets based only on the relative bias during their 16 months of overlap[16,17,30], as the latter record shows a temporal inhomogeneity in deviations from the temperature record (Fig. 2c,e). As discussed above, HALOE exhibits a low bias in the lower stratosphere during its final years of operation that may adversely affect a long-term data record constructed by merging HALOE with another data set such as Aura-MLS during this period. Our approach, in contrast, shows that taking the long-term behaviour of the data sets into account substantially improves the consistency between the water vapour and temperature records. After the strong dip around 2001, the previous mergeofHALOE and Aura-MLS only partiallyrecovers by 2010 (refs 26,30,31), whereas the merged record using CMAM30 recovers fully to pre-2001 values by 2007. Calculations of surface radiative forcing from changes in lower-stratospheric water vapour based on the simple merge of HALOE and Aura-MLS (ref. 30) may thus overestimate the cooling effect on global mean surface temperatures after 2001.

Comparison with *in-situ* observations over Boulder

We now turn to the question of the apparent inconsistency between the long-term Boulder FPH balloon and satellite data sets[15,17]. We investigate whether the Boulder trends are representative of the Northern Hemisphere mid-latitude stratosphere by sub-sampling the model at the location (40° N/105° W) and time of the Boulder measurements. Figure 3a shows Boulder 100 hPa water vapour anomalies extending back to 1980 together with the full and subsampled anomalies derived from the model. The agreement between the merged satellite and full model data sets back to 1988 provides confidence that the model exhibits a correct representation of interannual variability and long-term changes in stratospheric water vapour. The sub-sampled model fields generally correlate better with the Boulder *in-situ* measurements than do the full model fields in terms of year-to-year fluctuations, explaining the differences between the Boulder and (zonal-mean) satellite observations during some years (for example, 1988–1992, 1997–1998 and 2003–2005). Nevertheless, the 100 hPa change over 1980–2010 derived from the sub-sampled model fields (–0.27 ±0.18 ppmv) disagrees with that from Boulder (0.6 ± 0.15 ppmv). The difference is smaller, but still statistically significant (–0.15 ±0.22 ppmv compared with 0.39 ±0.18 ppmv), over 1988–2010 where the zonal-mean model trend is consistent with that of the merged satellite record. The differences from the near-global water vapour fields (Fig. 3b) illustrate in more detail the close agreement between the sub-sampled and Boulder water vapour records,

except for the three time periods highlighted in red, which together lead to the differences in their long-term trends. Inspection of the model's longitude–latitude distribution of water vapour changes indicates that these are not longitudinally uniform (Fig. 3c). Positive trends are found south-west of Boulder, with the limited spatial resolution of the model probably missing the full extent of the geographical structure and temporal variability of this feature. Our results suggest that the water vapour trends over Boulder should not be considered representative of the global stratosphere.

Long-term stratospheric water vapour changes

Figure 4a shows the bias-corrected individual water vapour data sets at 10hPa in the extratropics together with the model-instrument biases (Fig. 4b). Our method reveals minor discrepancies between two available SAGE II data versions (Supplementary Methods). HALOE shows no apparent low bias, as was identified in the lower stratosphere for its last years of operation, showing that satellite instrument biases and drifts can be altitude- and latitude-dependent. Although the model exhibits a strong low bias at this altitude, its long-term evolution and interannual variability show very good agreement with the observations back to 1986 (Fig. 4c). This level of agreement provides confidence in the ERA-Interim reanalysis driving the model while at the same time highlighting once again the high quality of the SAGE II data, suggesting that the satellite water vapour record can be extended back to the mid 1980s. (See Supplementary Fig. 3 for more examples.)

Figure 5a shows the long-term changes between the late 1980s and 2010 derived from the merged satellite record throughout the stratosphere, and Table 1 quantifies the long-term changes shown in the different figures. The trends are significantly positive in the upper stratosphere, whereas the lower and mid-stratosphere show significant negative trends (in contrast to the Boulder observations). This vertical structure in the long-term trends is found at all latitudes. In the tropical tropopause region around 80 hPa, a negative long-term trend is identified with 70% significance. On the other hand, positive changes of more than 10% are found in the tropical upper troposphere. Although these latter two findings need to be treated with caution owing to sampling limitations, they are in broad agreement with past trends derived from chemistry–climate model simulations[12,32].

The observed water vapour changes are now attributed to different drivers using the well-established 'total water' diagnostic[16,33,34] (Methods and Supplementary Methods). The contribution from methane entry-value changes is shown in Fig. 5b, and is derived from tropospheric observations of methane changes together with a fractional-release factor (a; Supplementary Fig. 3) inferred from ACE-FTS stratospheric methane measurements. The contribution varies smoothly from zero in the tropical lower stratosphere to approximately 3% of water vapour in the upper stratosphere, the latter representing a significant fraction of the observed water vapour increase (Fig. 5a). The contribution from water vapour entry-value changes is obtained from the merged 80 hPa record shown in Fig. 2a, and is a constant -0.14 ± 0.2 ppmv (hence not plotted). Assuming conservation of total water, the difference between the sum of those two contributions and the observed change can be attributed to changes in a, representing a change in stratospheric circulation, whose inferred contribution to the observed water vapour change is shown in Fig. 5c. This contribution is negative in the

lower stratosphere and positive in the upper stratosphere. The breakdown of the different contributions is shown in Fig. 5d together with their uncertainties for three locations with particularly large long-term water vapour changes.

The uncertainty in the inferred contribution from circulation changes is dominated by the large uncertainty in the water vapour entry-value changes because of the large interannual variability of the latter (Fig. 2a). However, the difference between the inferred contributions in the upper and lower stratosphere is robust because the same water vapour entry-value change is used for both, and it is not possible to explain the observed water vapour changes, within uncertainties, without the inferred circulation changes. In the northern high-latitude upper stratosphere (5 hPa, 62.5° N) the long-term increase of 0.28 ppmv is due in equal measure to methane increase and a increase, with an offset from the decreasing water vapour entry value. In the mid-latitude lower stratosphere of both hemispheres (30 hPa, 42.5° N and 50hPa, 42.5° S), long-term decreases of –0.28 and –0.34 ppmv respectively are mainly explained by decreasing a, with an additional contribution from the decreasing water vapour entry value and a small offset from the methane increase. Thus, the different drivers affect the water vapour changes differently in different regions.

Larger a corresponds to older age-of-air. To facilitate comparison with observed estimates of long-term circulation changes, we determine an approximate relationship between the two quantities (Supplementary Fig. 5), and use it to translate the inferred a changes into age-of-air changes (Fig. 5e). This shows a strong decrease in age-of-air in the lower stratosphere, and a weak increase in the upper stratosphere, which is broadly consistent with the evidence for both tendencies in long-term observations of stratospheric trace gases[35–37]. An increased strength of the lower-stratospheric circulation is also consistent with chemistry–climate model simulations[38], probably exacerbated in past decades by the effect of the ozone hole, which will reverse sign in the future[39].

Resolving the stratospheric water vapour conundrum

We have introduced a novel method to generate a long-term record of stratospheric water vapour, using a chemistry–climate model nudged to observed meteorology to provide a transfer function between the available satellite data sets. This approach provides an improved assessment of the relative biases between instruments, potential instrumental drifts, as well as possible sampling biases, compared to what is possible from the observations alone, especially for instruments with no or small overlap in time.

The new merged satellite water vapour record extends back to the late 1980s and shows long-term decreases in the lower and mid-stratosphere, in contrast to the Boulder record which is shown not to be globally representative. Upper-stratospheric water vapour instead shows a long-term increase. The contributions of the two recognized driversofwater vapour changes—the stratospheric entry values of water vapour and of methane—are quantified and shown not to be sufficient to explain the observed water vapour trends, particularly the difference in the trends between the upper and lower stratosphere. The discrepancy is attributed to changes in the fractional-release factor between methane and water vapour, which imply a strengthened lower-stratospheric circulation (reduced age-of-air) and a

weakened upper-stratospheric circulation (increased age-of-air), consistent with other evidence. It hence seems necessary to consider long-term changes in the stratospheric circulation when interpreting changes in stratospheric water vapour, together with changes in methane and water vapour entry values.

Our results show the value of using models and measurements together to understand the interannual and long-term behaviour of stratospheric water vapour, with the approach being applicable in principle to other trace gases. They also highlight the need for independent and redundant global measurement systems characterized by high long-term accuracy (and precision) to be able to quantify long-term changes in stratospheric water vapour with more confidence.

Methods

Nudged chemistry–climate model simulations

The CMAM30 data set is produced using the Canadian Middle Atmosphere Model[40] driven by the latest European Centre for Medium-Range Weather Forecasts (ECMWF) ERA-Interim reanalysis[21] over the past 30 years (1980-2010). For details on the nudging see Supplementary Methods. The model was run on 71 vertical levels from the surface to around 95 km, with a vertical resolution of approximately 1 km around the tropopause, and a horizontal resolution of T47, or approximately 4 degrees. The stratospheric source gas of water vapour, methane, is prescribed as a time-varying, global average surface concentration based on observations and is subject to model transport and chemistry. Water vapour is likewise a fully prognostic field in the model, chemically produced by methane oxidation and removed through parameterized large-scale and deep convective precipitation processes. Water vapour in excess of the local saturation mixing ratio is removed, following the rationale that the stratospheric water vapour entry value is largely determined by the Lagrangian cold point as air passes through the tropical tropopause[19], but neglecting super-saturation[41]. The free-running CMAM has been evaluated for its performance in the upper troposphere and lower stratosphere, both in the tropics[12] and extratropics[42], and found to be one of the best-performing models. CMAM30 data can be downloaded from www.cccma.ec.gc.ca/data/cmam/output/CMAM/CMAM30-SD/index.shtml.

SPARC Data Initiative time series

The SPARC Data Initiative water vapour time series have been compiled using profile data that were carefully screened before binning, and a hybrid log-linear interpolation in the vertical has been performed. The time series feature zonal monthly mean cross-sections with a horizontal resolution of 5° on 28 pressure levels between 300 and 0.1 hPa (around 64 km altitude). We here use the time series from seven instruments, which provide near-global coverage (SAGE II, HALOE, Odin/SMR, SCIAMACHY, ACE-FTS, Aura-MLS and MIPAS) and have been quality-assessed within the SPARC Data Initiative[23]. Sampling issues are discussed in ref. 43. The climatologies were based on the following data versions (specific references are provided in ref. 23): HALOE v19, SMR v2.0 (in the lower stratosphere) and SMR v2.1 (in the middle and upper stratosphere), SCIAMACHY v3.0, ACE-FTS v2.2, Aura-MLS v3.3, and MIPAS v3o_H_2O_13 (for 2002-2004 data) and

v5r_H$_2$O_220 (for 2005-2010 data, where the operation mode was switched from high-spectral to low-spectral resolution). SAGE II v6.2 submitted to the SPARC Data Initiative is only shown in Fig. 4, but otherwise is superseded by climatologies based on the improved SAGE II v7.0 data[44]. For methane, ACE-FTS data[45] were used. The SPARC Data Initiative climatologies can be downloaded from www.sparc-climate.org/data-center/data-access/sparc-data-initiative/.

Boulder balloon observations

Water vapour vertical profile measurements over Boulder by balloon-borne NOAA frost point hygrometers (FPHs) started in April 1980 and continue today. Most soundings were conducted monthly; however, the record contains several multi-month data gaps, especially above 22 km. A comparison of FPH and Aura-MLS measurements over Boulder and Lauder, New Zealand, shows no significant temporal drifts between the two instruments from 100 to 26hPa during 2004-2012 (ref. 46). See also discussion of measurement uncertainty in the Supplementary Methods.

Anomalies

Anomalies are calculated with respect to the full time period depicted in the different figures, by subtracting the seasonal cycle derived from each individual instrument or the model from the overall time series.

Trends and significance tests

Unless indicated otherwise, uncertainty estimates are given as two sigma throughout the manuscript. We use a least-square linear regression to derive the trends from deseasonalized water vapour anomaly time series at the different altitudes and latitudes. The significance of the trend is derived taking into account the effect of potential autocorrelation within the time series on the number of independent data points (reducing the effective sample size). This effective sample size is then used to recalculate the uncertainty of the derived trends and determine the tabulated one-sided student's t-test value, used to define the significance level of the trends. A more detailed discussion of the method can be found in ref. 47.

Total-water diagnostic

Apart from polar dehydration and other non-conservative processes, stratospheric 'total water' $H_2O + 2 \cdot CH_4$ is approximately conserved[16,33,34], hence water vapour and methane at a given location can be written as

$$H_2O = H_2O_{[e]} + 2\alpha CH_{4[e]}, CH_4 = (1-\alpha)CH_{4[e]} \quad (1)$$

where the subscript '[e]' refers to the entry value at the tropical tropopause (lagged by the mean age-of-air) and α represents a fractional-release factor which depends on the circulation. Under this assumption, (1) implies that sufficiently small water vapour changes can be attributed to changes in water vapour entry value, methane entry value and circulation according to

$$\Delta H_2O = \Delta H_2O_{[e]} + 2\alpha \Delta CH_{4[e]} + 2CH_{4[e]}\Delta \alpha \quad (2)$$

The calculation of α and $\Delta CH_{4[e]}$ and their uncertainties is described in the Supplementary Methods. The last term in (2) is calculated as a residual of the other terms that can be derived from observations, with its uncertainty being overwhelmingly dominated by that of $\Delta H_2O_{[e]}$. Hence the other uncertainties (including possible non-conservation of total water) are not critical.

Supplementary Material

Refer to Web version on PubMed Central for supplementary material.

Acknowledgments

References

1. Fu Q, et al. Contribution of stratospheric cooling to satellite-inferred tropospheric temperature trends. Nature. 2004; 429:55–58. [PubMed: 15129277]

2. Cowtan, K., Way, RG. Coverage bias in the HadCRUT4 temperature series and its impact on recent temperature trends. Q J R Meteorol Soc. 2014. http://dx.doi.org/10.1002/qj.2297

3. Forster PM, Shine KP. Stratospheric water vapour changes as a possible contributor to observed stratospheric cooling. Geophys Res Lett. 1999; 26:3309–3312.

4. Manabe S, Strickler RF. Thermal equilibrium of the atmosphere with a convective adjustment. J Atmos Sci. 1964; 21:361–385.

5. Forster PM, Shine KP. Assessing the climate impact of trends in stratospheric water vapor. Geophys Res Lett. 2002; 29:3309–3312.

6. Maycock AC, et al. The circulation response to idealized changes in stratospheric water vapor. J Clim. 2012; 26:545–561.

7. Riese M, et al. Impact of uncertainties in atmospheric mixing on simulated UTLS composition and related radiative effects. J Geophys Res. 2012; 117:D16305.

8. Oltmans SJ, et al. The increase in stratospheric water vapor from balloonborne, frostpoint hygrometer measurements at Washington, D.C., and Boulder, Colorado. Geophys Res Lett. 2000; 27:3453–3456.

9. Scherer M, et al. Trends and variability of midlatitude stratospheric water vapour deduced from the re-evaluated Boulder balloon series and HALOE. Atmos Chem Phys. 2008; 8:1391–1402.

10. Hurst D, et al. Stratospheric water vapor trends over Boulder, Colorado: Analysis of the 30 year Boulder record. J Geophys Res. 2011; 116:D02306.

11. Rohs S, et al. Long-term changes of methane and hydrogen in the stratosphere in the period 1978–2003 and their impact on the abundance of stratospheric watervapor. J Geophys Res. 2006; 111:D14315.

12. Gettelman A, et al. Multimodel assessment of the upper troposphere and lower stratosphere: Tropics and global trends. J Geophys Res. 2010; 115:D00M08.

13. Seidel DJ, et al. Climatological characteristics of the tropical tropopause as revealed by radiosondes. Geophys Res. 2001; 106:7857–7878.

14. Wang JS, Seidel DJ, Free M. How well do we know recent climate trends at the tropical tropopause? J Geophys Res. 2012; 117:D09118.

15. Randel WJ, et al. Interannual changes of stratospheric water vapor and correlations with tropical tropopause temperatures. J Atmos Sci. 2004; 61:2133–2148.

16. Fueglistaler S, et al. The relation between atmospheric humidity and temperature trends for stratospheric water. J Geophys Res. 2013; 118:1052–1074.

17. Randel WJ, Jensen EJ. Physical processes in the tropical tropopause layer and their roles in a changing climate. Nature Geosci. 2013; 6:169–176.

18. Hartmann, DL., et al. Climate Change 2013: The Physical Science Basis. Stocker, TF., et al., editors. Cambridge Univ. Press; 2013.

19. Fueglistaler S, Haynes PH. Control of interannual and longer-term variability of stratospheric water vapor. J Geophys Res. 2005; 110:D24108.

20. Fujiwara M, et al. Seasonal to decadal variations of water vapor in the tropical lower stratosphere observed with balloon-borne cryogenic frost point hygrometers. J Geophys Res. 2010; 115:D18304.

21. Dee DP, et al. The ERA-Interim reanalysis: Configuration and performance of the data assimilation system. Q J R Meteorol Soc. 2011; 137:553–597.

22. Voemel H, David DE, Smith K. Accuracy of tropospheric and stratospheric water vapor measurements by the cryogenic frost point hygrometer: Instrumental details and observations. J Geophys Res. 2007; 112:D08305.

23. Hegglin MI, et al. SPARC Data Initiative: Comparisons of water vapour climatologies from international satellite limb sounders. J Geophys Res. 2013; 118:11824–11846.

24. Simmons AJ, et al. Estimating low-frequency variability and trends in atmospheric temperature using ERA-Interim. Q J R Meteorol Soc. 2014; 140:329–353.

25. Thomason LW, et al. A revised water vapor product for the Stratospheric Aerosol and Gas Experiment (SAGE) II version 6.2 data set. J Geophys Res. 2004; 109:D06312.

26. Fueglistaler S. Stepwise changes in stratospheric water vapor? J Geophys Res. 2012; 117:D13302.

27. Rosenlof KH, Reid GC. Trends in the temperature and water vapor content of the tropical lower stratosphere: Sea surface connection. J Geophys Res. 2008; 113:D06107.

28. Randel, WJ. The Stratosphere: Dynamics, Transport and Chemistry. Polvani, S., Waugh, editors. American Geophysical Union; 2010. p. 123-135.

29. Kelly KK, et al. Dehydration in the lower Antarctic stratosphere during late winter and early spring, 1987. J Geophys Res. 1989; 94:11317–11357.

30. Solomon S, et al. Contributions of stratospheric water vapor changes to decadal variation in the rate of global warming. Science. 2010; 327:1219–1222. [PubMed: 20110466]

31. Jones A, et al. Evolution of stratospheric ozone and water vapour time series studied with satellite measurements. Atmos Chem Phys. 2012; 9:6055–6075.

32. Garfinkel CI, Waugh DW, Oman LD, Wang L, Hurwitz MM. Temperature trends in the tropical upper troposphere and lower stratosphere: Connections with sea surface temperatures and implications for water vapor and ozone. J Geophys Res. 2013; 118:9658–9672.

33. Le Texier H, Solomon S, Garcia RR. The role of molecular hydrogen and methane oxidation in the water vapor budget of the stratosphere. Q J R Meteorol Soc. 1988; 114:281–295.

34. Dessler AE, et al. An examination of the total hydrogen budget of the lower stratosphere. Geophys Res Lett. 1994; 21:2563–2566.

35. Ray EA, et al. Evidence for changes in stratospheric transport and mixing over the past three decades based on multiple data sets and tropical leaky pipe analysis. J Geophys Res. 2010; 115:D21304.

36. Engel A, et al. Age of stratospheric air unchanged within uncertainties over the past 30 years. Nature Geosci. 2009; 2:28–31.

37. Bönisch H, et al. On the structural changes in the Brewer–Dobson circulation after 2000. Atmos Chem Phys. 2011; 11:3937–3948.

38. Butchart N, et al. Chemistry–climate model simulations of twenty-first century stratospheric climate and circulation changes. J Clim. 2010; 23:5349–5374.

39. McLandress C, Shepherd TG. Simulated anthropogenic changes in the Brewer–Dobson circulation, including its extension to high latitudes. J Clim. 2009; 22:1516–1540.

40. Scinocca JF, et al. Technical Note: The CCCma third generation AGCM and its extension into the middle atmosphere. Atmos Chem Phys. 2008; 8:7055–7074.

41. Jensen EJ, et al. Ice nucleation and dehydration in the tropical tropopause layer. Proc Natl Acad Sci USA. 2013; 110:2041–2046. [PubMed: 23341619]

42. Hegglin MI, et al. Multimodel assessment of the upper troposphere and lower stratosphere: Extratropics. J Geophys Res. 2010; 115:D00M09.

43. Toohey M, et al. Characterizing sampling biases in the trace gas climatologies of the SPARC data initiative. J Geophys Res. 2013; 118:11847–11862.

44. Damadeo RP, et al. SAGE version 7.0 algorithm: Application to SAGE II. Atmos Meas Technol. 2013; 6:3539–3561.

45. De Mazière M, et al. Validation of ACE-FTS v2.2 methane profiles from the upper troposphere to the lower mesosphere. Atmos Chem Phys. 2008; 8:2421–2435.

46. Hurst DF, et al. Validation of Aura Microwave Limb Sounder stratospheric water vapor measurements by the NOAA frost point hygrometer. J Geophys Res. 2014; 119:1612–1625.

47. Santer BD, et al. Statistical significance of trends and trend differences in layer-average atmospheric temperature time series. J Geophys Res. 2000; 105:7337–7356.
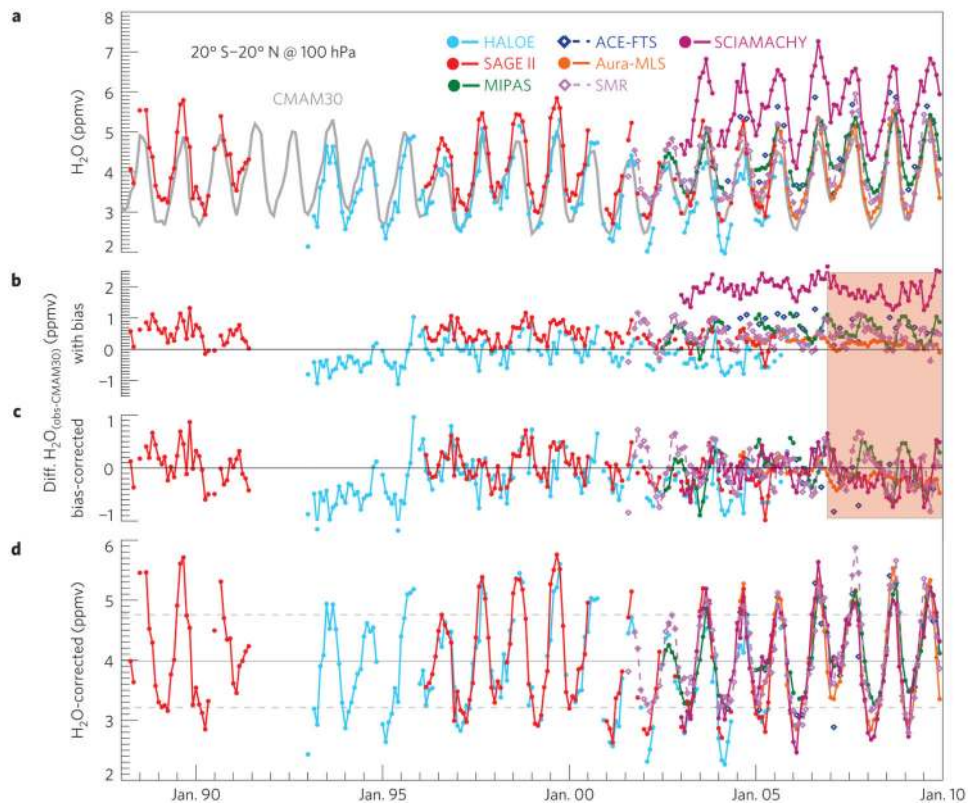
Figure 1. Approach to merging satellite data sets

Time series of monthly zonal mean water vapour at 100 hPa averaged over 20° S-20° N for 1988-2010. **a**, Absolute mixing ratios from different instruments (colours) and CMAM30 (grey). **b**-**d**, Differences (**b**), bias-corrected differences between observations and CMAM30 (**c**), and bias-corrected absolute mixing ratios from observations (**d**). Grey solid and dashed horizontal lines in **d** indicate mean and 1a (standard deviation) of the observational record averaged over the whole time period. The red box encompasses months excluded from the relative-bias determination owing to identified problems in ERA-Interim (see Text). See Supplementary Methods for SCIAMACHY bias explanation.
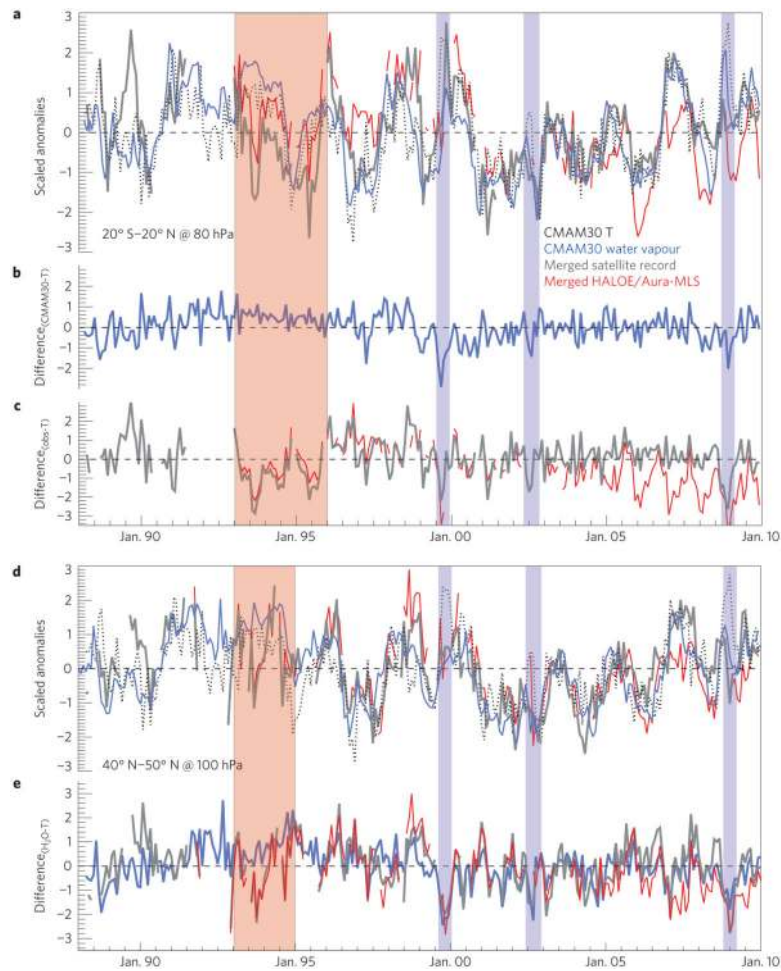
Figure 2. Consistency between tropical tropopause temperature and lower-stratospheric water vapour

a ,**d**, Scaled anomalies (unitless) of tropica temperature at 100 hPa averaged over 15° S-15° N (black dotted lines) and of water vapour at 80 hPa averaged over 20° S-20° N (**a**) and at 100 hPa averaged over 40° N-50° N (**d**). Tropical temperature is lagged by two (three) months in the tropics (extratropics). **b,c**, Differences between scaled water vapour and temperature anomalies (unitless) in the tropics for model (**b**) and merged satellite records (**c**). **e**, As in **b** and **c**, but for the extratropics. Red bar highlights a time period where the scaled anomalies in the model and the observations show a substantial disagreement, blue bars where the temperature-water vapour relationship is strongly perturbed in both model and observations.
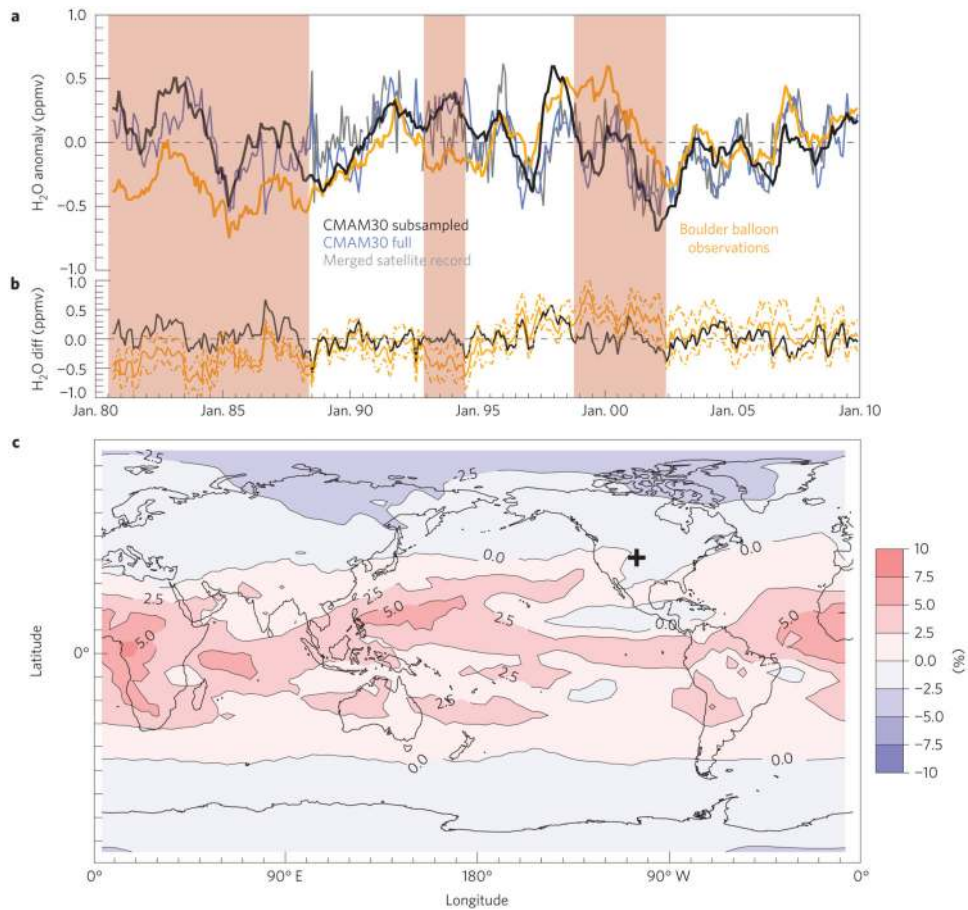
Figure 3. Comparison of stratospheric water vapour from Boulder balloon, model, and merged satellite records

a , Deseasonalized water vapour anomalies at 100 hPa derived from Boulder balloon observations (orange), the zonal mean (40° N-50° N) model (blue) and merged satellite data (grey), and the model subsampled at Boulder (black). **b**, Differences between full model anomalies and balloon (solid orange) or sub-sampled model anomalies (black). Red shading highlights periods where sub-sampled model data systematically lie outside the 1 桼 uncertainty of the balloon observations (dashed orange lines). **c**, Longitude-latitude percentage changes of water vapour at 100 hPa for 1980-2010 from the model. The cross indicates the location of Boulder (40° N/105°W).
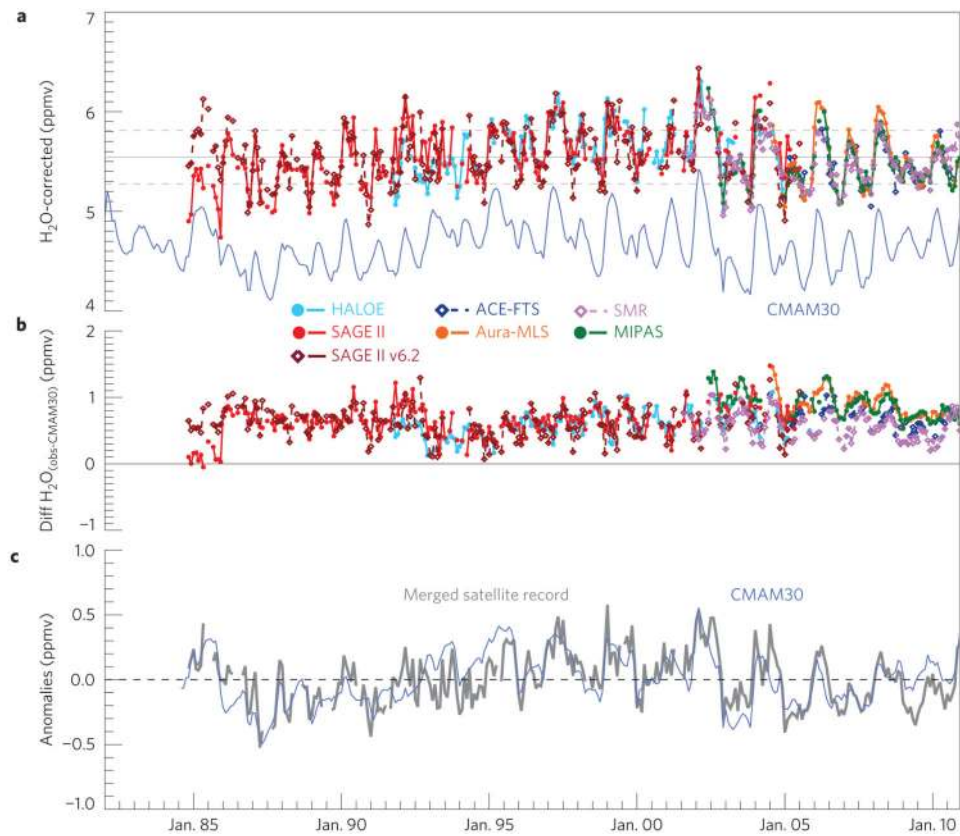
Figure 4. Extension of the water vapour time series back to the mid 1980s
a , Time series of zonal mean water vapour at 10 hPa and 40° N for model (blue) and the different instruments (bias-corrected and colour-coded). **b**, Relative biases between each instrument's original monthly zonal mean time series and CMAM30. **c**, Deseasonalized anomalies of the merged satellite water vapour record (grey) and the model.
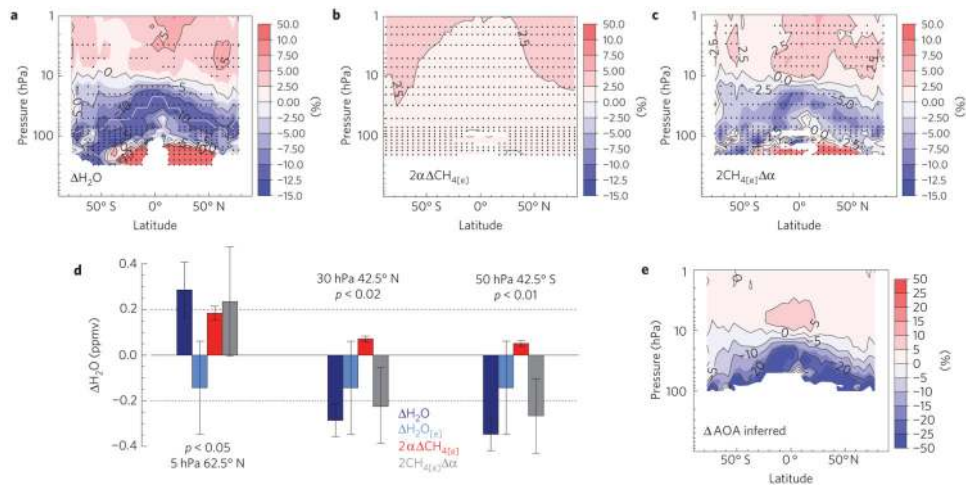
Figure 5. Long-term changes in stratospheric water vapour and its drivers
a , Percentage changes up to 2010 derived from the merged satellite record since 1986/1988 above/below grey line. Dots indicate 95%-significance level. **b,c**, Contribution to **a** from tropospheric methane increases (**b**) and inferred changes in the stratospheric circulation (**c**). **d**, Absolute water vapour changes at three locations and contributions from their drivers including uncertainties (as discussed in detail in Supplementary Methods). *p* values are given for the difference between observed changes and the sum of the two entry-value contributions. **e**, Fractional-release factor (α) changes translated into age-of-air (AOA) changes (significance not estimated).

Table 1

Water vapour and temperature changes derived for different time periods, latitude bands, and altitudes from observations and from CMAM30

H₂O data source	Period	Lat. band	Height (hPa)	Change (ppmv)	2σ uncertainty (ppmv)	t-value	Effective sample size	Significance level
Fig. 2 and Supplementary Fig. 2								
Satellite	1988–2010	20°S-20°N	80	−0.14	0.20	0.67	26	70%
Satellite	1988–2010	20°S-20°N	100	0.01	0.14	0.06	53	Not sig.
Fig. 3								
Satellite	1988–2010	40° N	100	−0.05	0.17	0.27	32	Not sig.
Boulder	1988–2010	40° N	100	0.39	0.18	2.17	129	95%
CMAM30ss	1988–2010	40° N	100	−0.15	0.22	0.66	84	Not sig.
CMAM30	1988–2010	40° N	100	−0.07	0.22	0.32	16	Not sig.
Boulder	1980–2010	40° N	100	0.60	0.15	3.9	160	95%
CMAM30ss	1980–2010	40° N	100	−0.27	0.18	1.49	110	90%
CMAM30	1980–2010	40° N	100	−0.12	0.19	0.64	22	Not sig.
Fig. 5d								
Satellite	1986–2010	62.5° N	5	0.28	0.12	2.4	26	95%
Satellite	1986–2010	42.5° N	30	−0.28	0.07	4.1	65	95%
Satellite	1986–2010	42.5° S	50	−0.34	0.07	5.2	72	95%

Temp. data source	Period	Lat. band	Height (hPa)	Change (K)	2σ uncertainty (K)	t-value	Effective sample size	Significance level
Fig. 2								
Model	1988–2010	15°S-15°N	100	−0.04	0.32	0.13	249	Not sig.

Changes are calculated for the time series shown in Fig. 2, Supplementary Fig. 2, Figs 3 and 5 and given as total change in ppmv or K over the entire period. Many trends are not statistically significant owing to large variability in stratospheric water vapour when compared to data record length. Decadal fluctuations strongly affect derived trend values, depending on the time period chosen[10,31]. Trend and significance calculation is explained in the Methods. CMAM30ss denotes sub-sampled model fields.